Chinese Chemical Letters 36 (2025) 110393

Contents lists available at ScienceDirect

Chinese Chemical Letters

journal homepage: www.elsevier.com/locate/cclet

Three-in-one reduction and acid-ignited micelles amplify antitumor efficacy *via* precise synergistic delivery of paclitaxel and naringenin

Yixin Sun[a,b], Keke Yu[a], Xiuchun Guo[a], Lanlan Zong[a,c,*], Zhonggui He[a,b,*], Xiaohui Pu[a,c,*]

[a] State Key Laboratory of Antiviral Drugs, Henan Province Engineering Research Center of High Value Utilization to Natural Medical Resource in Yellow River Basin, School of Pharmacy, Henan University, Kaifeng 475004, China
[b] Wuya College of Innovation, Shenyang Pharmaceutical University, Shenyang 110016, China
[c] Huaihe Hospital of Henan University, Kaifeng 475004, China

ARTICLE INFO

Article history:
Received 7 June 2024
Revised 29 August 2024
Accepted 30 August 2024
Available online 31 August 2024

Keywords:
Polymer prodrug micelles
Synergistic delivery
PTX
NAR
Cancer therapy

ABSTRACT

Chemotherapy is the cornerstone of cancer treatment, and paclitaxel (PTX), as a first-line broad-spectrum chemotherapy drug, is widely used in the treatment of multiple tumors in the clinic. However, unsatisfactory efficacy and drug resistance of single chemotherapy have severely hampered the clinical progress of PTX. Herein, three-in-one naringenin (NAR)-loaded PTX polymer prodrug micelles were constructed for efficient and synergistic antitumor therapy. Firstly, the polymer prodrug micelles could simultaneously act as nanoreservoirs for two hydrophobic drugs, PTX and NAR. Secondly, the polymer prodrug micelles enabled dual-responsive intelligent release of PTX and NAR triggered by reduction and acid. Finally, released PTX and NAR exerted synergistic antitumor effects for reversing tumor resistance, while NAR enhanced the immune and anti-inflammatory functions of polymer prodrug micelles. Due to the cascade-enhanced chemotherapeutic augmentation, the intelligent-responsive nanoreservoir proved to be an excellent antitumor therapeutic platform. This work was of great interest for designing superior chemotherapeutic augmentation regimens.

Cancer is becoming a major global public health problem threatening human health [1]. Chemotherapy is an essential cancer therapeutic approach in the clinic [2]. However, poor tumor selectivity, insufficient efficacy, and drug resistance greatly limit the clinical application of chemotherapeutic agents [3,4]. For example, paclitaxel (PTX), the first Food and Drug Administration (FDA)-approved chemotherapeutic agent derived from natural plants, is the first-line therapeutic agent for a wide range of cancers [5]. Nevertheless, the water solubility of PTX is extremely low (0.4 μg/mL), and the commercially available injection, Taxol, requires Cremphor EL and ethanol as solubilizers [6,7]. Notably, one of the patients treated with Taxol died of anaphylactic shock, which was sufficient to prevent further clinical studies of most of the drugs. Nanomedicines have shown enormous potential in cancer therapy due to the advantages of increasing drug solubility, prolonging blood circulation, enhancing tumor targeting, controllable drug release, and low toxicity compared to traditional formulations [8-11]. However, the currently marketed PTX nanoformulations only exhibit toxicity reduction but inferior potentiation. Therefore, how to reduce the toxicity while improving the therapeutic effect of PTX remains a challenge.

In recent years, flavonoid natural products have received widespread attention due to favorable safety and antitumor activity [12]. For example, naringenin (NAR), a flavonoid widely distributed in various fruits and herbs, has been found to exhibit a variety of biological activities, such as anticancer, anti-inflammatory, antioxidant, and immunomodulatory effects [13-17]. Moreover, NAR exhibits great potential for synergistic delivery with chemotherapeutic agents to improve therapeutic efficacy and reduce toxicity. However, NAR is a Biopharmaceutics Classification System (BCS) class II drug with poor solubility and low bioavailability [18]. The construction of innovative delivery systems to efficiently load and delivery of NAR and PTX is urgently needed.

Polymer micelles are drug delivery carriers with good stability and dispersion, which present unique advantages in cancer therapy [19-21]. Polymer micelles can be tailored with specific functions through chemical modifications, such as introducing disulfide bonds into the polymer [22-25]. Compared to normal cells, the high level of reductive microenvironment in tumor cells triggers the cleavage of disulfide bonds, enabling tumor-selective drug release [26-28]. However, the design of polymer micelles still suf-

* Corresponding authors.
E-mail addresses: lanlan198903@126.com (L. Zong), hezhgui_student@aliyun.com (Z. He), pgh425@163.com (X. Pu).

https://doi.org/10.1016/j.cclet.2024.110393
1001-8417/

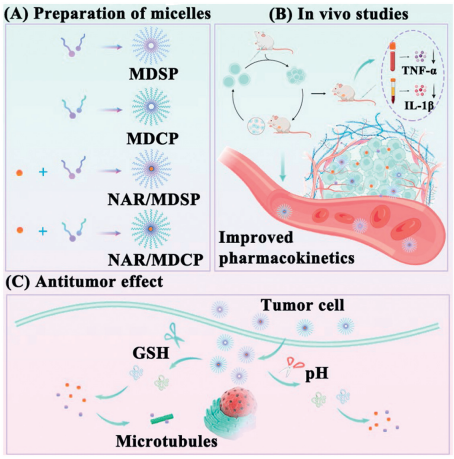

Scheme 1. PTX polymer prodrugs micelles were designed for loading NAR. The co-delivery of chemotherapeutic agents with anti-inflammatory and immune agents was expected to achieve multidimensional tumor suppression.

fers from the following concerns: (i) Polymers typically perform the role of carriers without the pharmacodynamic function. (ii) To realize the synergistic effect of two drugs, the commonly adopted strategy is loading two free drugs into the nanocarriers in a non-covalent form, which leads to the drawbacks of drug leakage and inability to synchronously release. Our preliminary study prepared polymer prodrug micelles (mPEG-DCA-SS-PTX/mPEG-DCA-CC-PTX) with antitumor efficacy and demonstrated that the micelles could overcome drug resistance [26-29]. Compared to single-modality therapy, combination therapy not only reduces the risk of drug resistance of tumor cells but also sensitizes chemotherapy through synergistic effects. In addition, the co-delivery of chemotherapeutic agents with anti-inflammatory and immune agents is expected to achieve multidimensional tumor suppression.

Based on the above issues, a disulfide bond-bridged PTX polymer prodrug was designed for loading NAR (NAR/mPEG-DCA-SS-PTX, NAR/MDSP), and the carbon bond-bridged PTX polymer prodrug was used as a control (NAR/mPEG-DCA-CC-PTX, NAR/MDCP). In addition, due to the covalent linkage of PTX to the polymer, investigating the fate of PTX polymer prodrug micelles without NAR could elucidate the function of PTX more clearly. The constructed polymer prodrug micelles offered the following advantages (Scheme 1): Firstly, the PTX polymer prodrug micelles could simultaneously serve as a stable nanoreservoir for two hydrophobic drugs, PTX and NAR. Secondly, the polymer prodrug micelles were reduction- and acid-responsive as well as resistant to multidrug resistance due to the presence of disulfide bonds and deoxycholic acid. Finally, the simultaneous release of PTX and NAR enhanced the synergistic antitumor effect. This three-in-one nanodelivery system implemented effective chemotherapeutic potentiation and the customized approach provided more possibilities for the design of nanoparticles, contributing to more efficient drug delivery and cancer therapy.

The structures and synthetic routes of mPEG-DCA-CC-PTX/mPEG-DCA-SS-PTX (MDCP/MDSP) polymer prodrugs were shown in Fig. 1A and Fig. S1 (Supporting information). The structures of MDCP/MDSP polymer prodrugs were corroborated and characterized in Figs. S2 and S3 (Supporting information). In addition, the synergistic effect of PTX and NAR was explored in PTX-resistant A549 cells. As shown in Fig. 1B and Table S1 (Supporting information), regardless of the ratio of PTX and NAR mixed within the screening concentration, the cytotoxicity was stronger than that of the PTX and NAR alone. The cytotoxicity of all groups increased progressively with increasing drug concentration. Moreover, PTX and NAR had a combination index (CI) $<$ 1 at mass ratios of 1:2, 1:1 and 2:1. In general, the CI $<$ 1 was considered synergistic. Therefore, PTX and NAR were significantly synergistic. Notably, the CI was the smallest (0.205) when the mass ratio of PTX and NAR was 2:1, suggesting that the antitumor effect of PTX and NAR on drug-resistant cells was stronger in this ratio. Therefore, the mass ratio of PTX and NAR of 2:1 was selected for the preparation and investigation of polymer prodrug micelles.

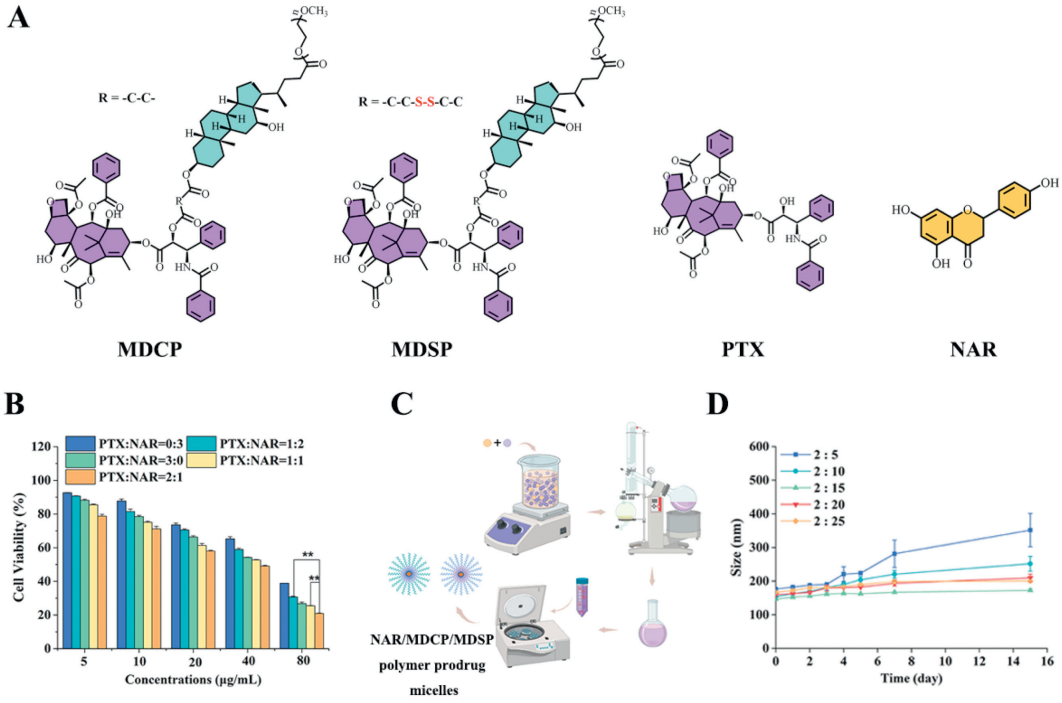

Fig. 1. (A) The structures of MDCP/MDSP polymer prodrugs, PTX and NAR. (B) Cell viability at different ratios of PTX and NAR (n = 2). $^{**}P < 0.01$ by two-tailed Student's t-test. (C, D) Preparation process and stability of polymer prodrug micelles at different feeding ratios (n = 3). Data are presented as mean ± standard deviation (SD).

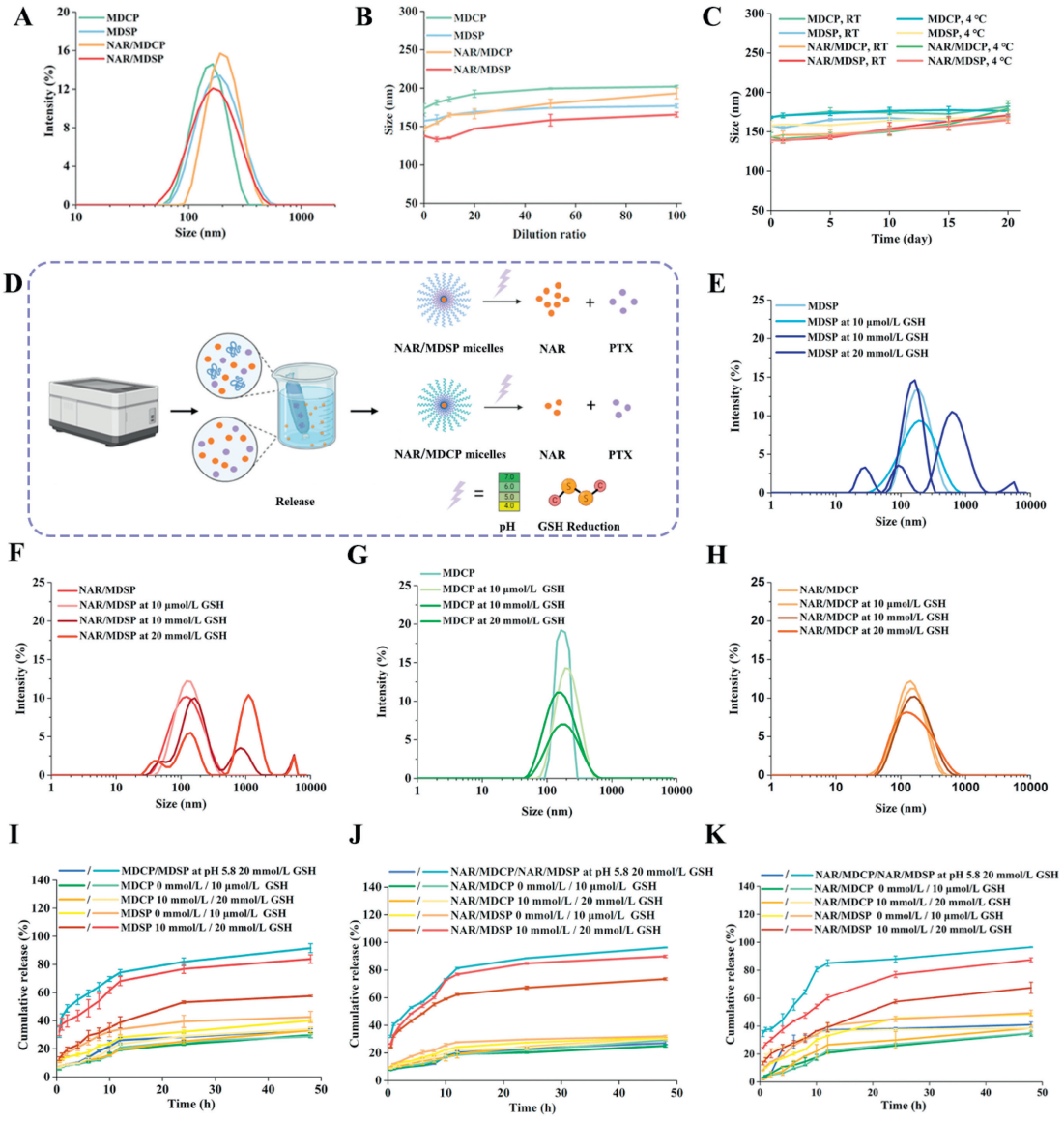

Fig. 2. (A) Particle sizes of MDCP, MDSP, NAR/MDCP and NAR/MDSP polymer prodrug micelles. (B) Dilution stability and (C) storage stability of MDCP, MDSP, NAR/MDCP and NAR/MDSP polymer prodrug micelles. (D) Reduction and acid-responsive release of MDCP, MDSP, NAR/MDCP and NAR/MDSP polymer prodrug micelles. (E–H) Changes in particle size of MDCP, MDSP, NAR/MDCP and NAR/MDSP polymer prodrug micelles in the presence of GSH. (I) PTX release from MDCP/MDSP polymer prodrug micelles at different concentrations of GSH and pH. (J) PTX and (K) NAR release from NAR/MDCP and NAR/MDSP polymer prodrug micelles at different concentrations of GSH and pH. Data are presented as mean ± SD ($n = 3$).

Subsequently, the optimal prescription was determined using single-factor analysis. Finally, the film dispersion method was selected for the preparation of polymer prodrug micelles. Methanol was used as the organic solvent and the preparation temperature was 45 °C (Tables S2–S9 in Supporting information). In addition, as shown in Figs. 1C and D, the best stability was obtained when the mass ratio of NAR:MDSP was 2:15. Therefore, the mass of MDSP polymer prodrug was set at 15 mg, which met the needs of both encapsulation efficiency and drug loading. As shown in Fig. 2A and Table S10 (Supporting information), the particle sizes of the polymer prodrug micelles were in the range of 140–170 nm, and the polydispersity index (PDI) was less than 0.3. Zeta potentials of NAR-loaded polymer prodrug micelles were −21 mV (NAR/MDCP) and −18 mV (NAR/MDSP), and the blank polymer prodrug micelles were −10 mV (MDCP) and −14 mV (MDSP), which could prevent the aggregation of particles by charge repulsion and improve the colloidal stability of micelles (Fig. S4 in Supporting information). Moreover, the uniform spherical shape of the polymer prodrug micelles was observed by transmission electron microscopy (Fig. S5 in Supporting information).

The dilution stability, storage stability, resolution stability and colloidal stability of polymer prodrug micelles were investigated. The particle sizes of MDCP, MDSP, NAR/MDCP and NAR/MDSP polymer prodrug micelles had no obvious change after 5, 10, 20, 50 and 100-fold dilution, indicating that the polymer prodrug micelles possessed satisfactory dilution stability (Fig. 2B). In addition, the changes in particle size were negligible when the polymer prodrug micelles were stored at 4 °C and room temperature for 20 days (Fig. 2C). The resolubilization stability of lyophilized powder of MDCP, MDSP, NAR/MDCP and NAR/MDSP polymer prodrug micelles was studied. As shown in Table S11 (Supporting information), the particle sizes of MDCP, MDSP, NAR/MDCP and NAR/MDSP polymer prodrug micelles were not significantly changed after lyophilization (without the addition of cryoprotectant). Meanwhile, the drug loading and encapsulation efficiency of NAR/MDCP and NAR/MDSP polymer prodrug micelles, as well as the drug loading of MDCP and

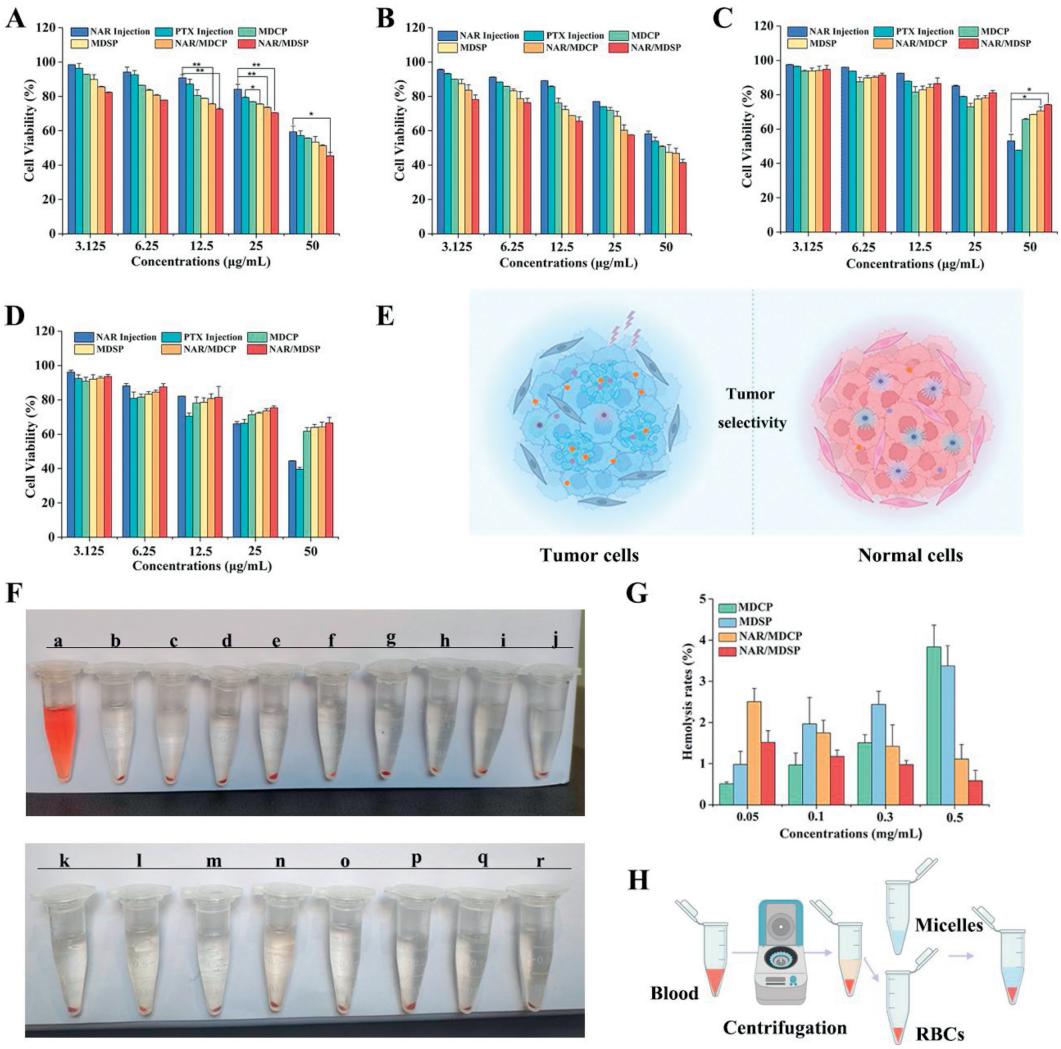

Fig. 3. (A–D) The cell viability of MDCP, MDSP, NAR/MDCP and NAR/MDSP polymer prodrug micelles on HepG2 tumor cells (A: 24 h; B: 48 h) and HL-7702 normal cells (C: 24 h; D: 48 h) ($n = 2$). $^{*}P < 0.05$, $^{**}P < 0.01$ by two-tailed Student's *t*-test. (E) Tumor selectivity of polymer prodrug micelles. (F) Photos of hemolysis experiment (a: distilled water, b: saline, c–f: 0.05–0.5 mg/mL MDCP, g–j: 0.05–0.5 mg/mL MDSP, k–n: 0.05–0.5 mg/mL NAR/MDCP, o–r: 0.05–0.5 mg/mL NAR/MDSP), (G) hemolysis rates ($n = 3$) and (H) experimental diagram. Data are presented as mean ± SD.

MDSP polymer prodrug micelles, were almost unchanged, which indicated that the structure of the polymer prodrug micelles was not damaged by the lyophilization process. Negligible changes in particle size were observed when the polymer prodrug micelles were incubated with PBS containing 10% fetal bovine serum (FBS) for 48 h, suggesting that the polymer prodrug micelles had good colloidal stability (Fig. S6 in Supporting information).

Effective release of PTX and NAR was essential for the efficacy of MDCP, MDSP, NAR/MDCP and NAR/MDSP polymer prodrug micelles. Therefore, the reduction release behavior of polymer prodrug micelles was investigated with glutathione (GSH) and acid as the triggering agents (Fig. 2D). Firstly, the reduction sensitivity of polymer prodrug micelles was qualitatively analyzed with the change in particle size. The particle sizes of the disulfide bond-containing MDSP and NAR/MDSP polymer prodrug micelles increased from 150 nm to 1000 nm in the presence of GSH (Figs. 2E and F), while the changes in the particle size of the non-reduction-sensitive MDCP and NAR/MDCP polymer prodrug micelles were negligible (Figs. 2G and H). Subsequently, the reduction release of PTX and NAR was quantitatively analyzed by high performance liquid chromatography (HPLC, Fig. S7 in Supporting information). As shown in Figs. 2I and J, the release of PTX from MDSP and NAR/MDSP polymer prodrug micelles increased gradually with increasing GSH concentration in the release medium at pH 7.4, while the release of PTX in MDCP and NAR/MDCP polymer prodrug micelles without disulfide bonds was less than 40%. Similarly, NAR release from NAR/MDSP polymer prodrug micelles increased with increasing GSH concentration in the same release medium, while NAR release from NAR/MDCP polymer prodrug micelles was less (Fig. 2K). In addition, MDCP/MDSP was reported to be acid-sensitive [29]. Thus, the release profiles of NAR/MDCP and NAR/MDSP polymer prodrug micelles were examined in a release medium (containing 20 mmol/L GSH) at pH 5.8. As shown in Figs. 2I–K, more PTX and NAR were released at pH 5.8 than at pH 7.4. Moreover, the cumulative release of PTX and NAR from NAR/MDSP polymer prodrug micelles reached about 94% at 48 h. Therefore, PTX and NAR could be released synchronously according to the synergistic ratio, showing a synergistic effect.

The cytotoxicity of MDCP, MDSP, NAR/MDCP and NAR/MDSP polymer prodrug micelles on tumor cells and normal cells was studied after identifying the effective release of PTX and NAR. For HepG2 tumor cells, the cytotoxicity of PTX injection, NAR injection, MDCP, MDSP, NAR/MDCP and NAR/MDSP polymer prodrug micelles was concentration and time-dependent (Figs. 3A and B).

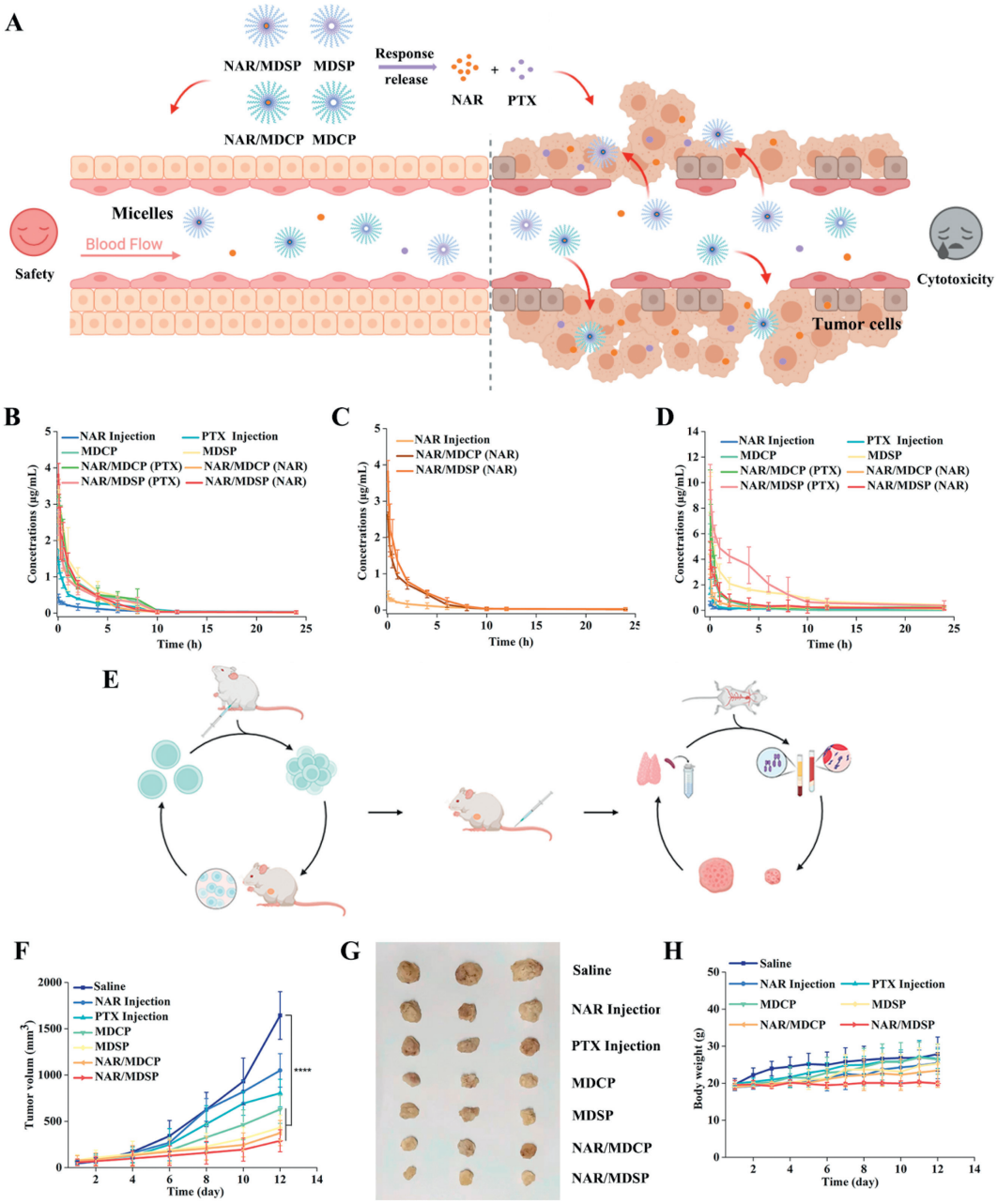

Fig. 4. (A) Pharmacodynamic studies. (B, C) Pharmacokinetic profiles of PTX injection, NAR injection, MDCP, MDSP, NAR/MDCP and NAR/MDSP polymer prodrug micelles. (D) Pharmacokinetic profiles of PTX injection, NAR injection, MDCP, MDSP, NAR/MDCP and NAR/MDSP polymer prodrug micelles after acid treatment ($n = 6$). (E) Pharmacodynamic operational procedures. (F) Changes in tumor volume and (G) body weight ($n = 10$). $^{****}P < 0.0001$ by two-tailed Student's *t*-test. (H) The photo of tumors in mice after treatment. Data are presented as mean ± SD.

With the increase in drug concentration and time, the cell viability of each formulation decreased significantly, and the cytotoxicity increased. Notably, NAR/MDCP and NAR/MDSP polymer prodrug micelles showed potent tumor cell killing ability compared to PTX injection and NAR injection, which might be due to the synergistic effect of NAR and PTX. For normal cells, the cytotoxicity of each formulation group was also concentration and time-dependent (Figs. 3C and D). Differently, MDCP, MDSP, NAR/MDCP and NAR/MDSP polymer prodrug micelles showed lower cytotoxicity than PTX injection and NAR injection for normal cells, which might be attributed to the lower reduction level and higher pH of normal cells than tumor cells. The cytotoxicity results indicated that polymer prodrug micelles possessed superior tumor selectivity and *in vivo* safety (Fig. 3E).

Before conducting *in vivo* experimental studies, it was necessary to investigate the blood compatibility of intravenously administered formulations, which was crucial to the safety. As shown in Figs. 3F–H, the hemolysis rates of MDCP, MDSP, NAR/MDCP and NAR/MDSP polymer prodrug micelles were less than 5% at different concentrations. These results revealed that the polymer prodrug micelles possessed good biocompatibility without destroying red blood cells as well as causing hemolysis.

Both PTX and NAR were hydrophobic and suffered from the disadvantages of limited drug delivery as well as rapid clearance. To investigate whether the polymer prodrug micelles could improve the *in vivo* fate of PTX and NAR, the pharmacokinetics of PTX injection, NAR injection, MDCP, MDSP, NAR/MDCP and NAR/MDSP polymer prodrug micelles were investigated (Fig. 4A). All animal

experiments were approved by the Ethics Committee for Animal Experimentation of Henan University. In pharmacokinetic experiments, precision test and extraction recovery rates of NAR and PTX in plasma samples were first validated (Table S12 in Supporting information). As shown in Figs. 4B, C and Tables S13, S14 (Supporting information), the area under the concentration-time curve (AUC) of MDCP, MDSP, NAR/MDCP and NAR/MDSP polymer prodrug micelles was increased by 1.8, 2.0, 1.8 and 2.6-fold, compared to PTX injection. Compared to the NAR injection, the AUC of NAR/MDCP and NAR/MDSP polymer prodrug micelles increased by 2.7 and 3.4-fold. Meanwhile, PTX and NAR were rapidly cleared after administration, whereas polymer prodrug micelles were effective in prolonging the retention time and improving the pharmacokinetic behavior of PTX and NAR. In addition, MDCP, MDSP, NAR/MDCP and NAR/MDSP polymer prodrug micelles were found to display acid sensitivity in the *in vitro* release. Therefore, the effect of acid treatment on the concentration of each formulation group was investigated in the pharmacokinetic experiments. Firstly, Table S15 (Supporting information) demonstrated that NAR and PTX were stable upon acid hydrolysis. As shown in Fig. 4D and Tables S16 and S17 (Supporting information), after acid treatment of plasma samples, the AUC of MDCP, MDSP, NAR/MDCP and NAR/MDSP polymer prodrug micelles were 3.6, 4.6, 3.5 and 5.9 times higher than that of PTX injection. The AUC of NAR/MDCP and NAR/MDSP were 9.0 and 17.7 times higher than that of the NAR injection. These results further demonstrated that MDCP, MDSP, NAR/MDCP and NAR/MDSP polymer prodrug micelles released less drugs within the systemic circulation and were expected to release more drugs within the acidic microenvironment of tumors. The pharmacokinetic results were consistent with the *in vitro* release, implying that the polymeric prodrug micelles possibly enhancing the antitumor effect while ensuring safety.

The stability, drug release, tumor selectivity and pharmacokinetics of polymer prodrug micelles affected the antitumor effect. Here, a tumor-bearing mice model was constructed to investigate the antitumor efficacy and mechanism of polymer prodrug micelles (Fig. 4E). As shown in Figs. 4F and G, PTX injection, NAR injection, MDCP, MDSP, NAR/MDCP and NAR/MDSP polymer prodrug micelles could inhibit tumor growth. Among them, PTX injection and NAR injection were weaker in tumor growth inhibition, followed by MDCP polymer prodrug micelles without NAR and disulfide bonds. In contrast, due to the high reduction and acid sensitivity, MDSP and NAR/MDSP polymer prodrug micelles exhibited potent antitumor effects. Notably, NAR/MDSP polymer prodrug micelles displayed the strongest antitumor effect, which could be attributed to the effective release and synergistic impacts of PTX and NAR.

Furthermore, NAR was reported to possess pharmacological activities such as immunomodulatory and anti-inflammatory. Therefore, the thymic index and splenic index of mice were examined after administration, and the levels of inflammatory factors (tumor necrosis factor-α (TNF-α) and interleukin-1β (IL-1β)) in tissues and serum were measured. As shown in Fig. S8 (Supporting information), the thymus index and spleen index of NAR/MDCP and NAR/MDSP polymer prodrug micelles were increased compared to PTX injection and NAR injection, indicating that NAR/MDCP and NAR/MDSP polymer prodrug micelles could enhance the immune function of mice (Table S18 in Supporting information). In addition, the results revealed that TNF-α and IL-1β were significantly reduced in tissues and serum of mice after administration of NAR/MDCP and NAR/MDSP polymer prodrug micelles, particularly in NAR/MDSP polymer prodrug micelles (Fig. S8). Therefore, the NAR/MDSP polymer prodrug micelles maximized the synergistic advantages of PTX and NAR and exhibited potent antitumor effects. Moreover, there was no significant decrease in the body weight of mice in the polymer prodrug micelle group, demonstrating good *in vivo* safety (Fig. 4H).

In summary, the customizable PTX polymer prodrugs were designed for loading NAR to strengthen the antitumor effect of chemotherapy. The *in vitro* and *in vivo* fate and antitumor mechanism of the polymer prodrug micelles were systematically investigated by sophisticated prescription screening, stability, responsive release, hemolysis tests, pharmacokinetics and pharmacodynamics. The following conclusions were drawn from the in-depth studies: Firstly, the polymer prodrug micelles could simultaneously serve as stable nanoreservoirs for two hydrophobic drugs. Secondly, the polymer prodrugs micelles were reduction- and acid-responsive as well as resistant to multidrug resistance due to the presence of disulfide bonds and deoxycholic acid. Finally, the simultaneous release of PTX and NAR enhanced the synergistic antitumor effect and immune function. The three-in-one nanodelivery system implemented effective chemotherapeutic potentiation and the polymer prodrug micelles with the best therapeutic effect were screened. This study overcame the dilemma of the unsatisfactory efficacy of existing nano-formulations, and the customized strategy provided a reference for the design of nanoparticles.

Declaration of competing interest

The authors declare that they have no known competing financial interests or personal relationships that could have appeared to influence the work reported in this paper.

CRediT authorship contribution statement

Yixin Sun: Writing – original draft, Methodology, Investigation. **Keke Yu:** Methodology, Investigation, Formal analysis, Conceptualization. **Xiuchun Guo:** Formal analysis, Data curation. **Lanlan Zong:** Writing – original draft, Data curation. **Zhonggui He:** Writing – review & editing, Conceptualization. **Xiaohui Pu:** Writing – review & editing, Supervision, Funding acquisition, Conceptualization.

Acknowledgments

This work was financially supported by the National Natural Science Foundation of China (No. U1904155), the Henan Provincial Key Research Development and Special Project for Promotion (Nos. 242102310455, 242102310473), the Key Project of Science and Technology Research funded by the Henan Provincial Department of Education (No. 24A350002), Postdoctoral Fellowship Program of CPSF (No. GZC20231732), China Postdoctoral Science Foundation (Nos. 2023TQ0222, 2023MD744229), General Program of Department of Education of Liaoning Province (No. JYTMS20231372), Doctoral Scientific Research Staring Foundation of Liaoning Province (No. 2024-BS-073).

Supplementary materials

Supplementary material associated with this article can be found, in the online version, at doi:10.1016/j.cclet.2024.110393.

References

[1] R.L. Siegel, A.N. Giaquinto, A. Jemal, CA Cancer J. Clin. 74 (2024) 12–49.
[2] Nat. Cancer 2 (2021) 245–246.
[3] J. Zhang, Y. Zhang, Y. Huang, et al., Chem. Eng. J. 458 (2023) 141510.
[4] Y. Tong, M. Gu, X. Luo, et al., J. Control. Release 363 (2023) 562–573.
[5] A.M. Sofias, M. Dunne, G. Storm, et al., Adv. Drug Deliv. Rev. 122 (2017) 20–30.
[6] S. Guo, M. Vieweger, K. Zhang, et al., Nat. Commun. 11 (2020) 972.
[7] Y. Sun, S. Wang, Y. Li, et al., Acta Biomater. 157 (2023) 417–427.
[8] T. Lammers, Adv. Mater. 36 (2024) 2312169.

[9] X. Zheng, X. Song, G. Zhu, et al., Adv. Mater. 36 (2024) 2308977.
[10] W. Jin, Z. Chen, Y. Wang, et al., Chin. Chem. Lett. 35 (2024) 109328.
[11] J. Huang, R. Kong, Y. Li, et al., Chin. Chem. Lett. 35 (2024) 109254.
[12] H. Zubair, M.A. Khan, S. Anand, et al., Semin. Cancer Biol. 80 (2022) 237–255.
[13] M. Motallebi, M. Bhia, H.F. Rajani, et al., Life Sci. 305 (2022) 120752.
[14] M. Amelimojarad, M. Amelimojarad, J. Wang, et al., Gene Rep. 26 (2022) 101532.
[15] J. Cai, H. Wen, H. Zhou, et al., Biomed. Pharmacother. 164 (2023) 114990.
[16] H. Zhang, Y. Li, J. Drug Deliv. Sci. Tec. 93 (2024) 105432.
[17] W. Zeng, L. Jin, F. Zhang, et al., Pharmacol. Res. 135 (2018) 122–126.
[18] R.L. Mianhong Chen, Y.Y. Gao, Y.Y. Zheng, et al., Foods 10 (2021) 963.
[19] L.L. Haidar, M. Bilek, B. Akhavan, Small 20 (2024) 2310876.
[20] Q. Zou, J. Huang, X. Zhang, Small 14 (2018) 1803101.
[21] A. Pitchaimani, T.D.T. Nguyen, R. Marasini, et al., Adv. Funct. Mater. 29 (2019) 1806817.
[22] P. Kanjilal, K. Dutta, S. Thayumanavan, Angew. Chem. Int. Ed. 61 (2022) e202209227.
[23] Z. Qin, Y. Yang, Q. Tian, et al., Chem. Eng. J. 467 (2023) 143434.
[24] Y. Qin, M. Huang, C. Huang, et al., Chin. Chem. Lett. 35 (2024) 109171.
[25] Y. Tao, C. Dai, Z. Xie, et al., Chin. Chem. Lett. 35 (2024) 109170.
[26] B. Sun, C. Luo, X. Zhang, et al., Nat. Commun. 10 (2019) 3211.
[27] S. Zheng, G. Li, S. Fu, et al., Chem. Eng. J. 479 (2024) 147802.
[28] H. Xu, S. Zuo, D. Wang, et al., J. Control. Release 360 (2023) 784–795.
[29] J. Du, L. Zong, M. Li, et al., Int. J. Nanomedicine 17 (2022) 1323–1341.